

Determination of doped charge density in superconducting cuprates from NMR or stripes

Manfred Bucher

Physics Department, California State University, Fresno,
Fresno, California 93740-8031

(Dated: December 3, 2020)

Abstract

Independent investigations of nuclear quadrupole resonance (NQR) and of stripes in high- T_c cuprates find a small deviation of doped-hole density h from the doping level of $La_{2-x}Sr_xCuO_4$. The value observed with NQR, $x - h \approx 0.02$, agrees closely with the density of itinerant holes, \tilde{p} , responsible for suppression of 3D-AFM, as obtained from stripe incommensurability. The stripe model's assumption that doped holes in $La_{2-x}Sr_xCuO_4$ reside at oxygen sites, and that doped electrons in $Ln_{2-x}Ce_xCuO_4$ ($Ln = Pr, Nd$) reside at copper sites, is (to a large degree) confirmed with NQR. The NQR finding of doped-hole probabilities in oxygen and copper orbitals of $HgBa_2CuO_{4+\delta}$ and other oxygen-enriched high- T_c cuprates, $P_p \simeq P_d \simeq 1/2$, as well as of oxygen-doped $YBa_2Cu_3O_{6+y}$, $P_p \simeq 2P_d \simeq 2/3$, is interpreted with the stripe model in terms of excess oxygen atoms in the CuO_2 planes and CuO chains.

I. INTRODUCTION

Superconductivity in doped copper oxides of high transition temperature (high T_c) occurs in the CuO_2 planes within certain doping ranges. When doped with heterovalent metal, such as hole-doped $La_{2-x}Sr_xCuO_4$ or electron-doped $Pr_{2-x}Ce_xCuO_4$, the doped-charge density in the CuO_2 planes is readily given by stoichiometry, $p = x$ and $n = x$, respectively. For oxygen-doped $YBa_2Cu_3O_{6+y}$, on the other hand, $p(y)$ cannot be inferred from stoichiometry because of simultaneous filling of CuO chains. Instead, one needs to resort to indirect methods. Most commonly used is the “universal-dome method” which obtains $p(y)$ from experimental data of $T_c(y)$ and $T_{c,max}$.¹ Because of its crucial role in superconductivity, independent methods to determine the doped-charge density are valuable. Two such methods are discussed and compared here—one using nuclear quadrupole resonance, the other one stripe incommensurability.

Nuclear quadrupole resonance (NQR) arises from the interaction of the quadrupole moment of nuclear charge distribution with the electric field gradient (EFG) at the nucleus. For nuclei of nonvanishing quadrupole moments, which holds for nuclear quantum numbers $I > \frac{1}{2}$, the method can provide information about the charge distribution in a compound. Particularly, with $I(^{43}Cu) = \frac{3}{2}$ and $I(^{17}O) = \frac{5}{2}$, NQR can give the doped-charge density in the CuO_2 planes. This was shown in a seminal paper by Haase *et al.* for $La_{2-x}Sr_xCuO_4$ and $YBa_2Cu_3O_{6+y}$ a decade and a half ago,² followed by the same treatment of oxygen-enriched cuprates and of electron-doped $Ln_{2-x}Ce_xCuO_{4+\delta}$ ($Ln = Pr, Nd$) a decade later.³⁻⁵

The doped-hole density p (and doped-electron density n) of high- T_c cuprates can also be determined from the incommensurability of charge-order and magnetization stripes, as shown in two recent papers.^{6,7} Shedding new light on the NQR results, here we point out commonalities with the stripe analysis, but also aspects that have been overlooked in the earlier studies or went unexplained.

II. NQR DETERMINATION OF DOPED-HOLE DENSITY IN $La_{2-x}Sr_xCuO_4$

Haase *et al.*² posit the NQR frequency at the oxygen nucleus, ν_O , to be proportional to the hole density n_p of the O $2p$ orbital,

$$\nu_O = Q_O \times n_p + C_O . \quad (1)$$

The coefficient Q_O is obtained from quantum-mechanical expressions of electric hyperfine interaction for isolated oxygen ions. Based on electron hopping parameters, n_p is determined for the undoped CuO_2 plane as $n_{p0} = 0.11$. Together with the experimental value of ν_O in the parent crystal, this enables the determination of the material-specific constant C_O . The NQR frequency of the Cu nucleus depends linearly on the hole density n_d of the $Cu 3d_{x^2-y^2}$ orbital, but also, by a cross-term, on neighboring $O 2p$ orbitals,

$$\nu_{Cu} = Q_{Cu} \times n_d - Q_{Cu}^O \times (8 - 4n_p) + C_{Cu} . \quad (2)$$

The coefficients Q_{Cu} and Q_{Cu}^O are obtained from quantum-mechanical expressions for isolated ions. With $n_{d0} = 1 - 2n_{p0} = 0.78$ for the undoped crystals, the constant C_{Cu} can be determined. For the *doped* crystals, Haase *et al.* make the assumption

$$h = n_d + 2n_p - 1 . \quad (3)$$

(In Ref. 2 the doped-hole density h is denoted as δ .) With experimental NQR frequencies ν_{Cu} and ν_O of $La_{2-x}Sr_xCuO_4$, along with the calculated coefficients and constants, the quantities n_d , n_p and h can be determined. They are listed in Table I. The doped-hole density h is close to the Sr -doping, $h \approx x$, which attests to the predictive power of the NQR approach. A closer look shows that h is systematically slightly lower than x ,

$$x - h = \Delta h \simeq 0.02 . \quad (4)$$

Is this an inaccuracy caused by the approximations involved or the result of some underlying physics? We shall return to this question.

The hole density in the $Cu 3d_{x^2-y^2}$ orbital arises from the contribution of the parent crystal and a doping-dependent term,

$$n_d = n_{d0} + P_d h . \quad (5)$$

Here P_d is the probability of a doped hole to reside at the Cu^{2+} ion. The corresponding expression for oxygen is

$$n_p = n_{p0} + \frac{1}{2} P_p h , \quad (6)$$

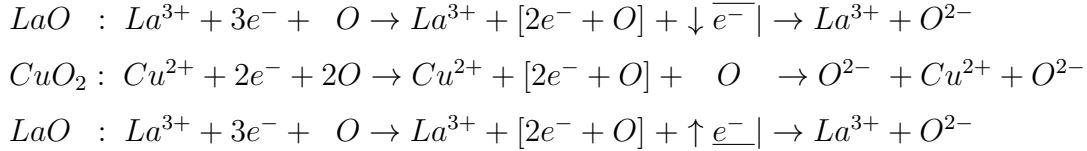
where the factor $1/2$ accounts for the *two* oxygen ions in the CuO_2 plane of the unit cell. From the data in Table I, $P_d \simeq 0.07$ and $P_p \simeq 0.93$ is obtained.² This shows that in $La_{2-x}Sr_xCuO_4$ the doped holes in the CuO_2 plane reside almost entirely at the oxygen sites—a conclusion that still holds in view of a small uncertainty of n_p , as the constant C_O in Eq. (1) can be determined only within bounds by the formalism of the NQR approach.⁴

x	ν_{Cu} [MHz]	ν_O [MHz]	n_d	n_p	h	$x - h$	\tilde{p}
0.00	33.2	0.147	0.780	0.110	0.00	0.00	
0.075	34.2	0.18	0.784	0.137	0.058	0.017	0.020
0.10	34.6	0.195	0.785	0.149	0.084	0.016	0.015
0.15	35.8	0.215	0.794	0.166	0.125	0.025	0.015
0.20	36.6	0.245	0.797	0.190	0.190	0.023	0.015
0.24	37.4	0.28	0.798	0.219	0.236	0.004	0.015

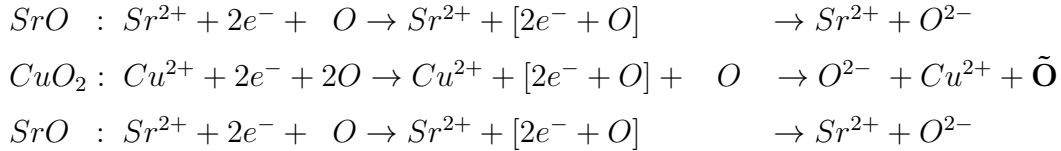
TABLE I: NQR frequencies ν_{Cu} and ν_O , hole density n_d and n_p in $Cu\ 3d_{x^2-y^2}$ and $O\ 2p_c$ orbitals, respectively, and density h of doped holes in the CuO_2 plane of $La_{2-x}Sr_xCuO_4$, obtained from NQR data (Ref. 2); difference from nominal Sr doping, $x - h$; and density of itinerant holes, \tilde{p} , from stripe incommensurability, Ref. 6.

III. STRIPES IN $La_{2-x}Sr_xCuO_4$

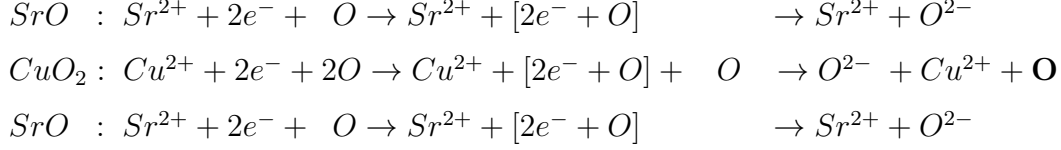
The unit cell of *pristine* La_2CuO_4 has a central CuO_2 plane, sandwiched by LaO planes. Consider stepwise ionization, where brackets indicate electron localization at atoms, both within the planes and by transfer from the LaO planes to the CuO_2 plane:



In the simplest case of *doping*, Sr substitutes, in some cells, La in both sandwiching planes:



The lack of electron transfer from the sandwiching planes to the CuO_2 plane leaves some oxygen atoms *neutral* (marked bold above and below). Compared to the host crystal, they can be regarded as housing the holes (pairwise).⁶ Up to a doping density $\tilde{p} \leq 0.02$, such holes are *itinerant*, enabling \tilde{O} atoms to skirmish long-range antiferromagnetism (3D-AFM).⁶ The remaining lack of electron transfer leaves more oxygen atoms *stationary* at lattice sites, O . They give rise to static stripes.



Relative to the host crystal, both the skirmishing and stationary oxygen atoms, \tilde{O} and O , appear positive, holding two elementary charges, $+2|e|$, each. In this sense, the doping of La_2CuO_4 with Sr is often called “hole doping” (more accurately, doping the CuO_2 planes with holes). Both the \tilde{O} and O atoms have a finite magnetic moment, $\mathbf{m}(\tilde{O}) = \mathbf{m}(O) \neq 0$, due to their spin quantum number $S = 2 \times \frac{1}{2} = 1$ according to the spin configuration $[\uparrow\downarrow] [\uparrow] [\uparrow]$ of their $2p^4$ subshell (Hund’s rule of maximal multiplicity). The moments of the skirmishing oxygen atoms, $\mathbf{m}(\tilde{O})$ —itinerant *via* anion lattice sites—upset the 3D-AFM the host [from $\mathbf{m}(Cu^{2+})$ moments] and cause its collapse at hole density $\tilde{p} = 0.02$.

The superlattice, formed by the O ions, gives rise to charge-order stripes. Their incommensurability, in reciprocal lattice units (r.l.u.), depends on Sr -doping x ,

$$q_c(x) = \frac{\Omega^\pm}{2} \sqrt{x - \tilde{p}}, \quad x \leq \hat{x}, \quad (7)$$

up to a “watershed” doping \hat{x} .⁶ The stripe-orientation factor is $\Omega^+ = \sqrt{2}$ for $x > 0.056$ when stripes are parallel to the a or b axis, but $\Omega^- = 1$ for $x < x_6$ when stripes are diagonal. The offset value under the radical is $\tilde{p} \leq 0.02$. A qualitative change of the incommensurability occurs at a watershed concentration of the dopant, \hat{x} , which depends on the species of doping and co-doping. It shows up as *kinks* in the $q_c(x)$ profile at \hat{x} (see Fig. 1), where the square-root curve from Eq.(7) levels off to constant plateaus,

$$q_c(x) = \frac{\sqrt{2}}{2} \sqrt{\hat{x} - \tilde{p}}, \quad x > \hat{x}. \quad (8)$$

The charge-order stripes are accompanied by magnetization stripes of incommensurability $q_m(x) = \frac{1}{2}q_c(x)$. The square-root dependence of $q_c(x)$ results from the spreading of the double holes by Coulomb repulsion to the farthest available separations. Thus a rising square-root profile of stripe incommensurability signifies an underlying superlattice of *lattice-defect charges* (relative to the host crystal). Increasing density of the doped holes, housing pairwise at lattice-defect O atoms in the CuO_2 planes, raises their Coulomb repulsion energy. When doping exceeds a watershed value, $x > \hat{x}$, additional holes overflow to the LaO planes⁶ where they also reside pairwise in O atoms. This leaves charge-order stripes of *constant* q_c in the CuO_2 planes, Eq. (8).

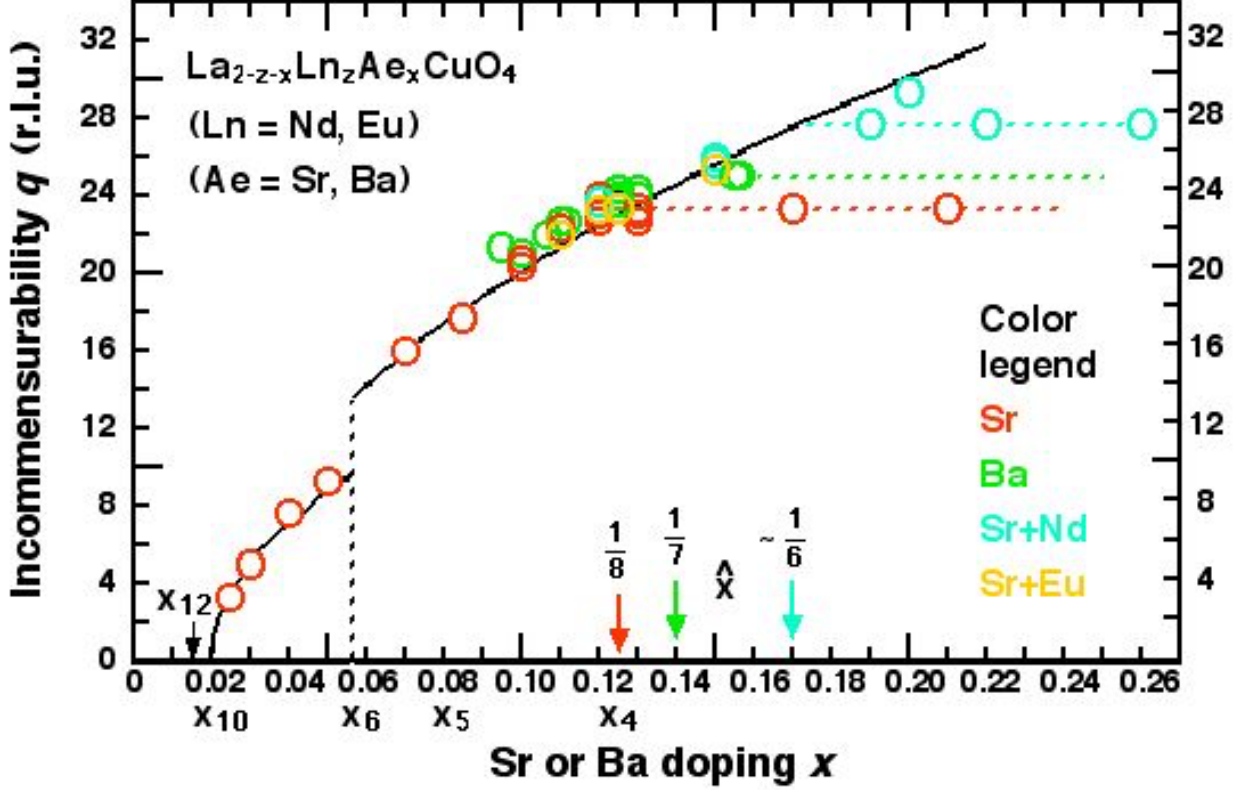


FIG. 1. Incommensurability of charge-order stripes, $q = q_c$, and of magnetization stripes, $q = 2q_m$, in $La_{2-z-x}Ln_zAe_xCuO_4$ ($Ln = Nd, Eu; z = 0, 0.4, 0.2$) due to doping with $Ae = Sr$ or Ba . Circles show data from X-ray diffraction or neutron scattering. The broken solid curve is a graph of Eq. (7). The discontinuity at $x = 0.056$ is caused by a change of stripe orientation from diagonal to parallel, relative to the $Cu-O$ bonds. Doping beyond watershed concentrations, \hat{x} , yields constant stripe incommensurabilities, given by Eq. (8) (dashed horizontal lines).

IV. COMMONALITIES IN THE STRIPE AND NQR STUDIES OF $La_{2-x}Sr_xCuO_4$

The stripe model assumes that the density of doped holes in the CuO_2 plane equals the Sr -doping, $p = x$. However, it distinguishes between itinerant holes of density \tilde{p} and stationary holes of density $x - \tilde{p}$, located pairwise in the O atoms of the oxygen superlattice. The distinction between both kind of holes is inferred from the collapse of long-range antiferromagnetism (3D-AFM) when Sr -doping reaches the Néel concentration, $x = x_{N0} = 0.02$, at vanishing Néel temperature, $T_N(x_{N0}) \equiv 0$, and from stripe incommensurability, Eq. (7). As Fig. 1 shows, a large host of data from neutron scattering, hard X-ray diffraction, and resonant soft X-ray scattering is well described by Eq. (7). For low temperatures and

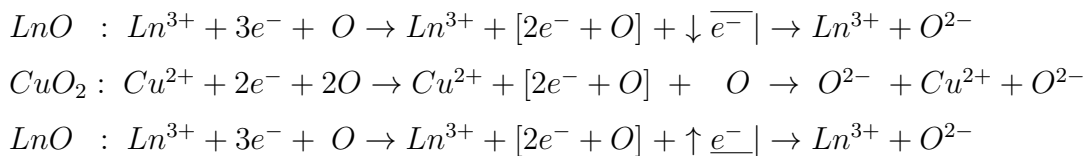
low doping ($x < 0.09$), the offset value \tilde{p} in Eq. (7) agrees with the Néel concentration, $\tilde{p} = x_{N0} = 0.02$. With more *Sr* doping, but still at $T \approx 0$, it is found that a *smaller* value, $\tilde{p} < x_{N0}$, suffices to keep 3D-AFM suppressed.⁶ Thus the use of $\tilde{p} = 0.02$ in Eq. (7) becomes inaccurate beyond the low doping range, $x > 0.09$, as it gives *too small* a value for the incommensurability $q_{c,m}(x)$. This can be seen in Fig. 1 where in that range most data points cluster slightly above the drawn $q(x)$ curve. Use of a *diminished* offset value, $\tilde{p} \simeq 0.015$ in this range (confirmed by recent measurements, as discussed in Ref. 6) shifts that section of the curve slightly upward to better agreement with experiment (not shown).

Returning to the NQR method, the close agreement of the doped hole density h with *Sr*-doping of $La_{2-x}Sr_xCuO_4$, $h \approx x$, confirms the validity of the approach. Even better is the systematic slight deviation Δh , Eq. (4), to which no significance may have been attributed previously. As only *stationary* holes would contribute, via EFG, to NQR signals, the NQR method should detect a doped-hole density $x - \tilde{p}$. This strongly suggests the identification $\Delta h = \tilde{p}$, relating to *itinerant* holes. Residing pairwise in skirmishing \tilde{O} atoms, they lead to suppression of 3D-AFM when $x = x_{N0} = 0.02$ and keep 3D-AFM suppressed for $x > x_{N0}$. The values of $x - h$ and \tilde{p} in Table I scatter somewhat about $x_{N0} = 0.02$, possibly due to underlying approximations. (The $x - h$ value for $x = 0.24$ —from the heavily overdoped range—defies the trend.)

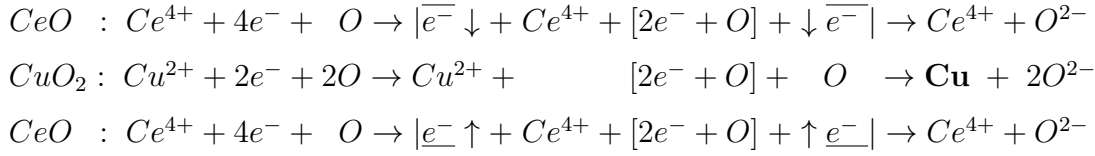
Since the NQR method^{2,3} assumes an *average* hole density h in the CuO_2 plane, Eq. 3, it cannot discriminate whether the doped holes reside singularly in O^- ions or doubly in O atoms. The finding from stripe analysis of *double holes* in O atoms awaits confirmation (or refutation) by other experiments.

V. NQR AND STRIPES IN n-DOPED $Ln_{2-x}Ce_xCuO_4$, $Ln = Pr, Nd$

The unit cell of *pristine* Ln_2CuO_4 ($Ln = Pr, Nd$) has a central CuO_2 plane, sandwiched by LnO planes, analogous to La_2CuO_4 . Consider again crystal formation by stepwise ionization, where brackets indicate electron localization at atoms, both within the planes and by transfer from the LnO planes to the CuO_2 plane:



In the simplest case of *doping*, *Ce* substitutes, in some cells, *Ln* in both sandwiching planes:



Doping lanthanide-based cuprates with cerium, $Ln_{2-x}Ce_xCuO_4$, partially substitutes Ln^{3+} by Ce^{4+} , resulting in *electron doping* of the CuO_2 plane. As there are *no* itinerant doped electrons in the CuO_2 plane, the doped-electron density equals the *Ce*-doping,

$$n = x . \quad (9)$$

The doped electrons reside pairwise in lattice-site \mathbf{Cu} atoms.⁶ Relative to the host crystal, the Cu atoms have a lattice-defect charge of $-2|e|$. Coulomb repulsion spreads the Cu atoms to form a Cu superlattice. Its charge-order incommensurability is given by Eq. (7), with $\tilde{p} = \tilde{n} = 0$ (see Fig. 2).

A consequence of smaller ionic radius, $r(Pr^{3+}, Nd^{3+}) \simeq 1.26 \text{ \AA}$, compared to $r(La^{3+}) = 1.30 \text{ \AA}$, the $Ln_{2-x}Ce_xCuO_4$ compounds have the T' crystal structure. It differs from the T structure of $La_{2-x}Sr_xCuO_4$ by the position of the O^{2-} ions in the layers that bracket the

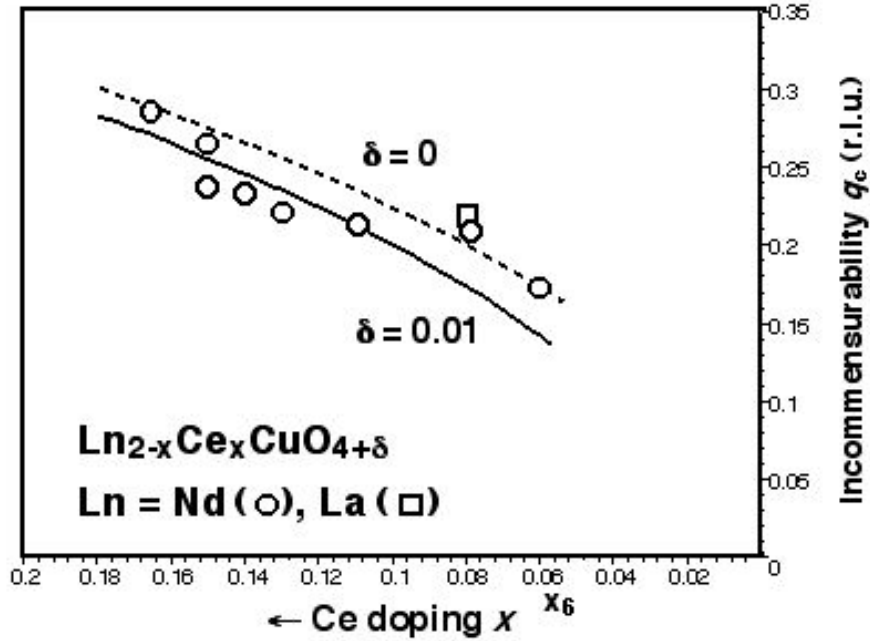


FIG. 2. Observed incommensurability q_c of charge-order stripes in $Ln_{2-x}Ce_xCuO_{4+y}$, $Ln = Nd, La$ (see Ref. 6). The curves are graphs of Eq. (7) without excess oxygen ($\delta = 0$, dashed line) and with excess oxygen of $\delta = 0.01$ (solid line).

CuO_2 plane. In the T structure those O^{2-} ions are at apical positions (above or beneath the Cu^{2+} ions) whereas in the T' structure they reside above or beneath O^{2-} ions of the CuO_2 plane. As a result, the unit cell of the parent crystal Ln_2CuO_4 is wider and shorter ($a \simeq 3.95 \text{ \AA}$, $c \simeq 12.19 \text{ \AA}$) than of La_2CuO_4 ($a = 3.81 \text{ \AA}$, $c = 13.2 \text{ \AA}$).⁸

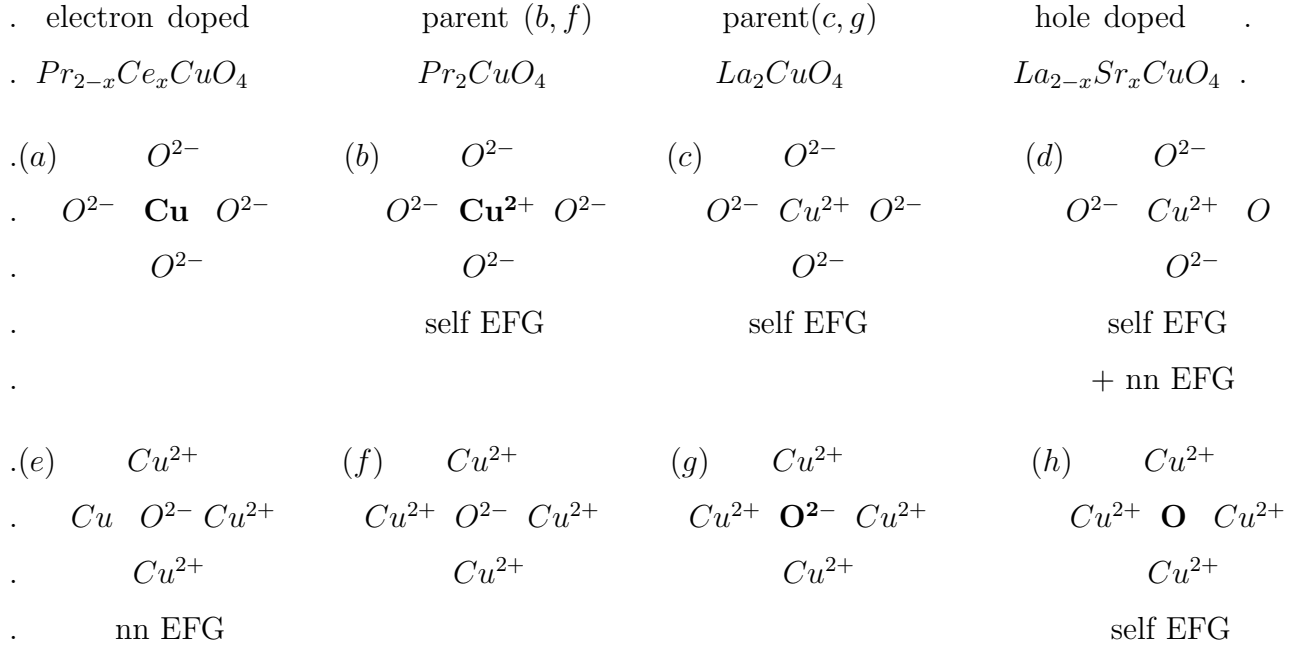
For reasons of stability, $Ln_{2-x}Ce_xCuO_4$ crystals need to be grown with excess oxygen, O_δ , to be eliminated in post-growth annealing.⁸ As Eq. (7) is based on Coulomb repulsion of like charges in the CuO_2 planes, its success for stripes in electron-doped ‘214’ compounds (of T' structure) implies that the excess oxygen must reside interstitially as oxygen ions, O_δ^{2-} , in or between the LnO planes.⁶ Any residual excess oxygen results in a *hole*-doping contribution to the CuO_2 planes that correspondingly reduces their electron-doping from Ce . Accordingly, the charge-order incommensurability of $Ln_{2-x}Ce_xCuO_{4+\delta}$ can be expressed with Eq. (7) using $\tilde{p} = 2\delta$.⁶

The NQR investigations of $Ln_{2-x}Ce_xCuO_4$ yield doped-electron densities very close to the Ce -doping, approximating Eq. (9).^{4,5} It is found that doping with electrons predominantly decreases n_d but only slightly n_p . In other words, the doped electrons in $Ln_{2-x}Ce_xCuO_4$ reside almost entirely at Cu atoms. The copper signal ν_{Cu} is very sensitive to Ce -doping, having a wide background of broadened satellites such that the signal effectively disappears at $x = 0.15$. For oxygen, the NQR analysis obtains a hole content $n_p \simeq 0.20$ in the parent Ln_2CuO_4 compounds, compared to $n_p \simeq 0.10$ in La_2CuO_4 .

A comparative interpretation of the NQR results from hole-doped and electron-doped cuprates is complicated by several factors:⁹⁻¹¹ (i) the EFG at a copper or oxygen nucleus from a hole in its own electron shell (here called “self EFG”); (ii) the EFG from differently charged nearest neighbors in the CuO_2 plane (abbreviated “nn EFG”); (iii) the presence or absence of O^{2-} ions above and beneath Cu^{2+} ions—called “apical” oxygen ions—and of O^{2-} above and beneath O^{2-} ions in the CuO_2 plane according to the T or T' structure; (iv) hybridization of $Cu 3d_{x^2-y^2}$ and $O 2p_\sigma$ orbitals leading to covalent bond, (v) deformation of electron shells in the crystal, and (vi) higher-order effects.

Using the finding from the stripe model that doped holes and electrons are hosted *pairwise* in O and Cu atoms, respectively, the following diagrams provide a qualitative overview of possible cases with combinations of the influences (i), (ii) and (iii). The top diagrams show planar configurations of the copper sites and the bottom diagrams those of the oxygen sites. The middle panels give the configurations in the parent crystals and the outer panels those

of the doped sites. The largest effect on NQR can be expected from self EFG, noted beneath the corresponding diagrams. (No self EFG exists at the Cu nucleus due to the spherical $4d^{10}5s^1$ orbitals of the atom.) Noticeable effects can also be expected from planar nn EFG and from the presence or absence of nearest neighbors in the sandwiching layers according to the compounds' T or T' structure. Here the **absence** of O^{2-} above and beneath Cu^{2+} and Cu in Pr_2CuO_4 and $Pr_{2-x}Ce_xCuO_4$, respectively, is marked bold in the diagrams (b, a). Likewise, the **absence** of O^{2-} ions above and beneath O^{2-} and, respectively, O in the CuO_2 plane of La_2CuO_4 is marked bold in (g, h). In all cases the effects of undoped and doped sites are different. Thus it is not surprising that the corresponding NQR frequencies are different. This renders a comparison difficult.



VI. NQR DETERMINATION OF DOPED-HOLE DENSITY IN $YBa_2Cu_3O_{6+y}$

Using the same procedure as for $La_{2-x}Sr_xCuO_4$, Haase *et al.*² obtain for $YBa_2Cu_3O_{6+y}$ the doped-hole densities h listed in Table II. The results are comparable with values from the universal-dome method and from stripe incommensurability.^{1,7} This confirms again the validity of the NQR approach to determine h . However, in striking contrast to the heterovalent-metal-doped compounds, $La_{2-x}Sr_xCuO_4$ and $Ln_{2-x}Ce_xCuO_4$ ($Ln = Pr, Nd$), where the doped holes and electrons were found to reside almost entirely at oxygen and, respectively, copper ions, distinctly different orbital occupancies are found with NQR for oxygen-doped

TABLE II: Doped-hole density h in $YBa_2Cu_3O_{6+y}$, obtained from NQR data for copper d and oxygen p_c orbitals,² from stripe incommensurability,⁷ and from the universal dome method.¹

y	$h \leftarrow$ NQR	$h \leftarrow$ Stripes	$h \leftarrow$ Universal Dome
0.00			0.00
0.31		0.00	0.05
0.45		0.07	0.08
0.50	0.00	0.09	0.08
0.60	0.10	0.12	0.09
0.63	0.11	0.13	0.10
0.68	0.14	0.14	0.12
0.75		0.16	0.14
0.92		0.18	0.16
0.96	0.16		0.19

and oxygen-enriched compounds.³⁻⁵ With Eqs. (5, 6) one can obtain the orbital probabilities P_d and P_p , according to which a doped hole resides at a copper or oxygen ion in the CuO_2 plane, by the slope,

$$s = \frac{n_d - n_{d0}}{2n_p - 2n_{p0}} = \frac{P_d}{P_p}, \quad (10)$$

of orbital-occupation data in an n_d vs. $2n_p$ display. Together with $P_d + P_p \equiv 1$, this gives

$$P_d = \frac{s}{s+1} \quad \text{and} \quad P_p = \frac{1}{s+1}. \quad (11)$$

In Fig. 5 of Ref. 4 the n_d vs. $2n_p$ values fall along straight lines for compounds families. Their slopes are listed in Table III along with a doped hole's orbital-occupation probabilities. In oxygen-doped $YBa_2Cu_3O_{6+y}$ and $YBa_2Cu_4O_8$, $P_d \approx \frac{1}{3}$ and $P_p \approx \frac{2}{3}$ is found. In oxygen-enriched *Hg*-, *Bi*-, and *Tl*-based cuprates, they are essentially equal, $P_d \simeq P_p \simeq \frac{1}{2}$. How can these findings be understood and what do they tell us?

VII. STRIPES IN $YBa_2Cu_3O_{6+y}$

The unit cell of $YBa_2Cu_3O_{6+y}$ has two CuO_2 planes, separated by the Y plane and bracketed by BaO layers. At the top (and bottom) of each unit cell of *undoped* $YBa_2Cu_3O_6$

TABLE III: Slopes s of orbital-occupation data from Ref. 4, Fig. 5, and occupation probabilities P_d and P_p of doped copper d and oxygen p_σ orbitals for heterovalent-metal-doped cuprates (upper part) and oxygen-doped/enriched cuprates (lower part).

Compound	s	P_d	P_p
$La_{2-x}Sr_xCuO_4$	0.14	0.12	0.88
$Pr_{2-x}Ce_xCuO_4$	4.82	0.83	0.17
$Nd_{2-x}Ce_xCuO_4$	6.50	0.87	0.13
$YBa_2Cu_3O_{6+y}$, $YBa_2Cu_4O_8$	0.55	0.36	0.64
$HgBa_2CuO_{4+\delta}$, $Bi_2Ba_2CaCu_2O_{8+\delta}$,	0.96	0.49	0.51
$Tl_2Ba_2CuO_{6+\delta}$, $Tl_2Ba_2CaCu_2O_{8+\delta}$, $Tl_2Ba_2Ca_2Cu_3O_{10+\delta}$	0.96	0.49	0.51

is a plane of Cu^+ ions (called the “ $Cu(1)$ plane”). In order to introduce the effects of doping we temporarily make a simplifying assumption (here called the “0.5-watershed”), that we’ll later drop when more familiar. By this approximation, oxygen doping $y \leq 0.5$ causes ionization in the $Cu(1)$ plane, $O + 2Cu^+ \rightarrow 2Cu^{2+} + O^{2-}$, with the O^{2-} ions residing between Cu^{2+} ions along the crystal’s b direction, called CuO chains. The CuO_2 planes remain unaffected by this doping. Accordingly *no* charge-order stripes are observed for $y \leq 0.5$. The filling of $Cu^{2+}O^{2-}$ chains is completed at doping $y = 0.5$, as can be seen by stoichiometry and charge balance of $Y^{3+}Ba_2^{2+}Cu_3^{2+}O_{6.5}^{2-}$. The $Cu(1)$ plane of $YBa_2Cu_3O_{6.5}$ alternates with filled and empty CuO chains (called “ortho-II oxygen ordered”).

By the 0.5-watershed approximation, doping $y > 0.5$ causes incorporation of O atoms either in more CuO chains of the $Cu(1)$ plane or in the $CuO_2 \equiv Cu(2)$ planes,

$$y = \chi^{Cu(1)}(y) + 2\delta^{Cu(2)}(y). \quad (12)$$

It is the density of embedded oxygen, $\delta^{Cu(2)} \equiv \delta$, in each CuO_2 plane that gives rise to charge-order stripes. Their incommensurability [averaged over stripes along the a and b direction, $\bar{q}_c = (q_c^a + q_c^b)/2$], is given by the empirical formula⁷

$$\bar{q}_c(y) = \bar{q}_c(y_c^{ons}) - \gamma \times [\delta(y) - \delta(y_c^{ons})]. \quad (13)$$

Here the superscript ‘*ons*’ indicates the onset of charge-order (c) stripes. The onset incommensurability is material-specific: $\bar{q}_c(y_c^{ons}) = 0.33$ for $YBa_2Cu_3O_{6+y}$. Both the coefficient $\gamma = 0.64/\text{r.l.u.}$ and the onset density $\delta(y_c^{ons}) = 0.035$ hold for the whole family of oxygen-

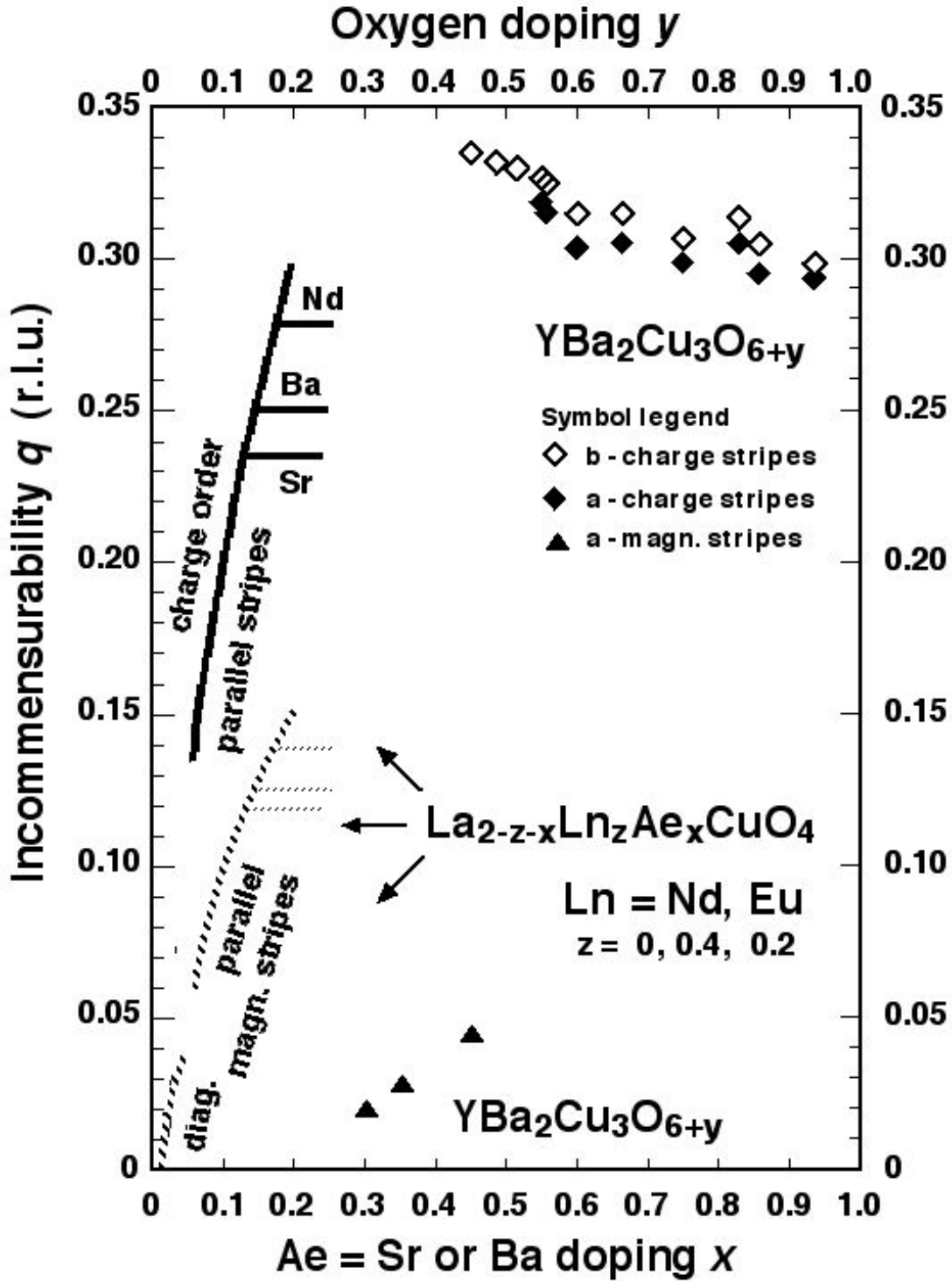


FIG. 3. Incommensurability of charge-order stripes (solid line) and magnetization stripes (hatched line) in $La_{2-z-x}Ln_zAe_xCuO_4$ of the ‘214’ family due to Ae doping with $Ae = Sr$ or Ba (curves on the left, equivalent to Fig. 1) and in oxygen-doped $YBa_2Cu_3O_{6+y}$ near the top (and near the bottom, if insufficiently annealed).

doped/enriched cuprates.⁷ Figure 3 shows the observed incommensurabilities of charge-order stripes (q_c^a and q_c^b), in $YBa_2Cu_3O_{6+y}$ (and q_m^a of magnetization stripes if the crystals are not sufficiently annealed—not discussed here). For comparison, the (re-scaled) result from Fig. 1 is included in Fig. 3 on the left. The doping dependence of charge-order stripes is distinctly different in the alkaline-earth-doped cuprates, $La_{2-x}Ae_xCuO_4$ ($Ae = Sr, Ba$), and in the oxygen-doped cuprate, $YBa_2Cu_3O_{6+y}$, showing a square-root dependence of the former, Eq. (7), but almost constant values of the latter, Eq. (13). The square-root dependence results from Coulomb repulsion of the doped holes in the CuO_2 plane (residing pairwise in lattice-site O atoms) to the largest separation, causing formation of an O superlattice. Conversely, the almost constant $q_c(y)$ values of $YBa_2Cu_3O_{6+y}$ result from the implementation of *neutral* O atoms in the CuO_2 planes. (The slight decrease of $q_c(y)$ with increasing O -doping y is caused by secondary effects.⁷) The distinctly different doping dependence of charge-order incommensurability disproves the common misconception that doped oxygen ionizes in $YBa_2Cu_3O_{6+y}$ as $O_y \rightarrow O^{2-} + 2e^+$ and separates—with O^{2-} entering the so-called charge-reservoir layer (that is, all planes except CuO_2) and the holes, $2e^+$, entering the CuO_2 planes. If this were true, then a rising square-root doping dependence of charge-order stripes in $YBa_2Cu_3O_{6+y}$ would result, *contrary* to the observed $q_c(y) \approx const.$ ⁷

It has been proposed⁷ that each doped oxygen atom is embedded in the CuO_2 plane at an interstitial site between four O^{2-} ions, called “pore” (see Fig. 4). The oxygen atom at the pore site, denoted $\overset{\circ}{O}$, bonds with two O^{2-} neighbors (abbreviated as $\ddot{O} \equiv O^{2-}$) to form an ozone molecule ion, $\ddot{O}\overset{\circ}{O}\ddot{O}$. Linked by an intermediate oxygen ion each (marked bold, $\mathbf{\ddot{O}}$), the ozone molecules line up along the crystal’s a or b direction to form trains of $\ddot{O}\overset{\circ}{O}\ddot{O}\mathbf{\ddot{O}}$ motifs that are observed as charge-order stripes in the CuO_2 planes of oxygen-doped $YBa_2Cu_3O_{6+y}$ and $YBa_2Cu_4O_8$, as well as of oxygen-enriched, $HgBaCuO_{4+\delta}$, and the *Bi*- and *Tl*-based cuprates.⁷ The distinction of oxygen-*doping* y , and oxygen-*enrichment* δ , signifies the stoichiometric exactitude of y , in contrast to the uncertainty of δ due to diffusive procedures and thermal treatment. For $YBa_2Cu_3O_{6+y}$, the doping certainty is of little help, however, when it comes to the oxygen content of the CuO_2 planes as the doped oxygen is shared to an uncertain degree with the CuO chains, Eq. (12).

The “0.5-watershed” simplification, employed for ease of introduction, holds *approximately*, but not strictly: To a small degree, O atoms are already embedded in the CuO_2 planes for $y < 0.5$ —weak charge-order stripes are already observed in the doping range

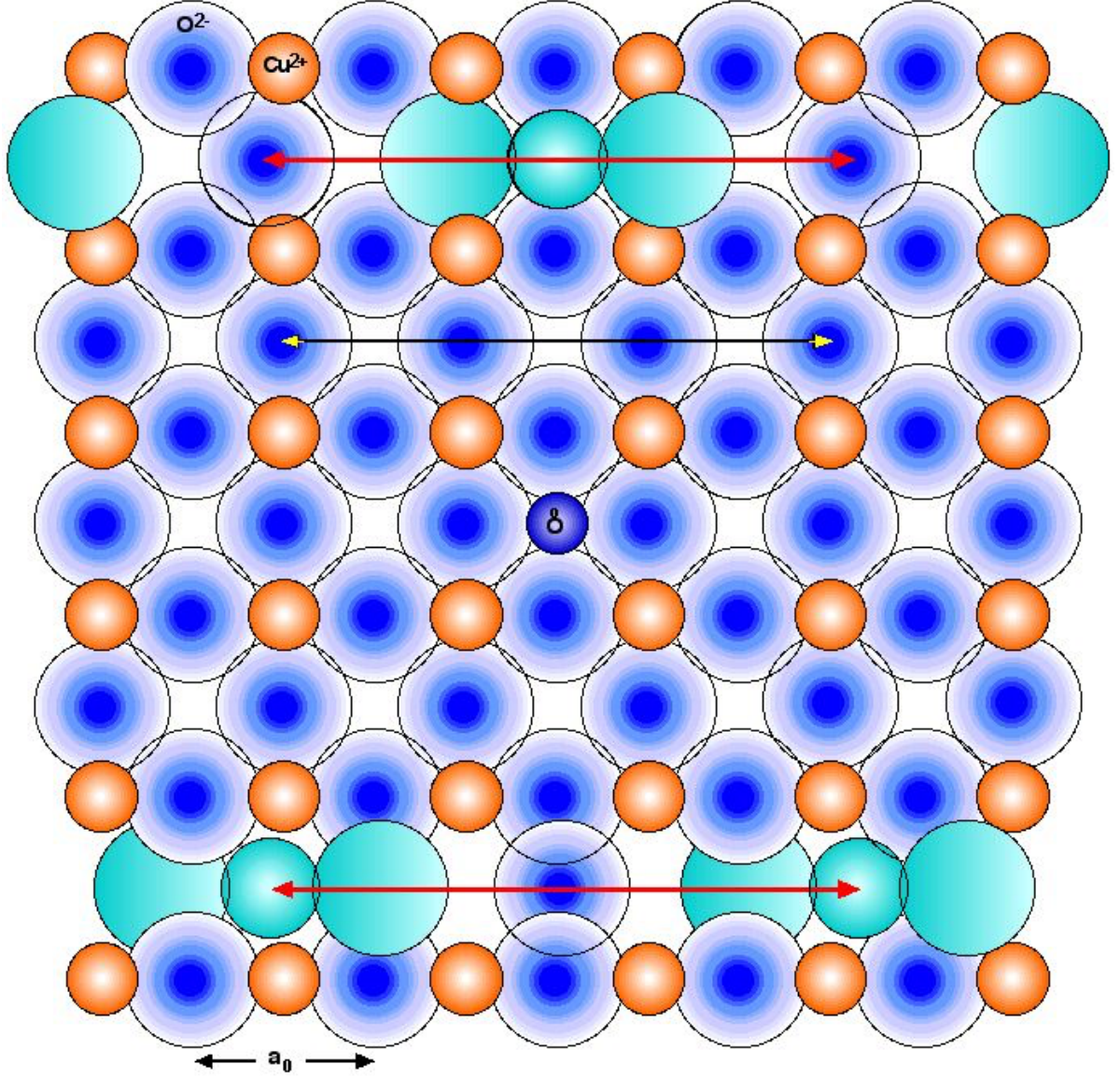


FIG. 4. Doped oxygen in the CuO_2 plane of $YBa_2Cu_3O_{6+y}$ ($y \simeq 0.55$), shown schematically for an oxygen atom at the stages of embedding (center, sixth row) and final relaxation (second row top and bottom). In the space (“pore”) between four O^{2-} ions (denoted \ddot{O} for short), the embedded oxygen atom (denoted \dot{O}) bonds with two O^{2-} neighbors, here in the a -direction, to form an ozone molecule ion, $\ddot{O}\dot{O}\ddot{O}$ (turquoise color). Linked by an intermediate oxygen ion each (marked bold, $\ddot{\ddot{O}}$), the ozone molecules line up to form trains of $\ddot{O}\dot{O}\ddot{O}$ motifs. The length of a motif is $L \simeq 3.125 a_0$ (red double arrow), slightly larger than $3a_0$ (black double arrow). Its reciprocal gives the incommensurability of charge-order stripes, $q_c = 1/L \simeq 0.32$ r.l.u.

$0.45 < y < 0.5$, and low- T_c superconductivity in $0.31 < y < 0.5$. Accordingly, some CuO chain filling with O^{2-} ions continues for $y > 0.5$ besides the then prevalent filling with O atoms.

VIII. COMPARISON OF STRIPE AND NQR STUDIES OF HIGH- T_c CUPRATES

The relevant properties of heterovalent-metal-doped and oxygen-enriched cuprates are given in Table IV. The hole-doped example of $La_{2-x}Sr_xCuO_4$ suffices for the comparison, as electron-doped cases correspond equivalently (see table caption). In order to avoid complications from CuO chain filling in oxygen-doped $YBa_2Cu_3O_{6+y}$, we compare with oxygen-enriched $HgBa_2CuO_{4+\delta}$, where *all* excess oxygen is embedded in the CuO_2 plane.

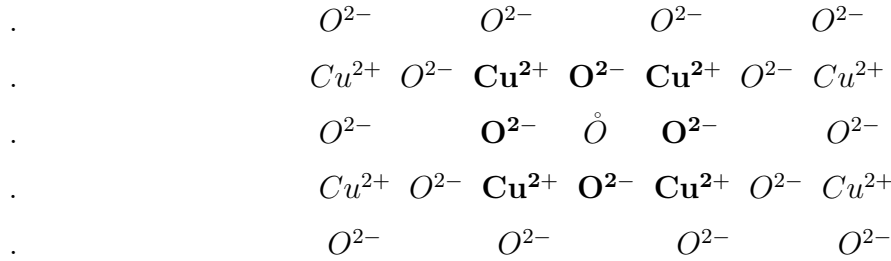
The outstanding distinction is a hole-doping of the CuO_2 plane of $La_{2-x}Sr_xCuO_4$, with holes residing pairwise at lattice-site O atoms, but of neutral O -atom-embedding in $HgBa_2CuO_{4+\delta}$, located at interstitial positions (“pores”). Strictly speaking, calling the

Property	hole-doped	oxygen-enriched
Example compound	$La_{2-x}Sr_xCuO_4$	$HgBa_2CuO_{4+\delta}$
Doping/enrichment of the crystal with causes doping of the CuO_2 plane with	Sr e^+	O \mathring{O}
Net charge accumulation in CuO_2 plane?	yes	no
From stripe analysis:	$2e^+ + \underline{O}^{2-} \rightarrow \underline{O}$	$O \rightarrow \mathring{O}$
Location of doping-affected oxygen	at <u>lattice site</u>	at interstitial position
Defect charge of doping-affected oxygen	$\underline{Q} = 2 e $	$\mathring{Q} = 0$
Coulomb repulsion of Q's?	yes	no
Stripe incommensurability	$q_c(x) \propto \sqrt{x - \bar{p}}$	$q_c(\delta) \approx const.$
NQR: doped orbital probability	$P_d \approx \frac{1}{8}, P_p \approx \frac{7}{8}$	$P_d \simeq P_p \simeq \frac{1}{2}$
NQR interpretation:	doped holes \rightarrow latt.-site oxy.	?

TABLE IV: Comparison of hole-doped and oxygen-enriched cuprates. Electron-doped cases correspond equivalently to hole-doping with replacements $La_{2-x}Sr_xCuO_4 \rightarrow Pr_{2-x}Ce_xCuO_4; Sr \rightarrow Ce; e^+ \rightarrow e^-; 2e^+ + \underline{O}^{2-} \rightarrow \underline{O} \Rightarrow 2e^- + \underline{Cu}^{2+} \rightarrow \underline{Cu}; \underline{Q} \rightarrow -2|e|; P_d \rightarrow \frac{6}{7}, P_p \rightarrow \frac{1}{6}$; doped electrons \rightarrow lattice-site copper.

presence of excess oxygen, O_δ , in the CuO_2 plane “hole doping” is a misnomer—“oxygen-atom doping” would be a more accurate (although awkward) term. Despite their common lack of two electrons from a closed $2p^6$ shell, lattice-site \underline{O} atoms and interstitial $\overset{\circ}{O}$ atoms have different properties due to their different position in the crystal. In $La_{2-x}Sr_xCuO_4$, Coulomb repulsion spreads the effective defect-charges of the lattice-site oxygen, $\underline{Q} = 2|e|$, to an O superlattice which gives rise to charge-order stripes. Their incommensurability has a rising square-root dependence on Sr doping x . In contrast, the excess $\overset{\circ}{O}$ atoms in $HgBa_2CuO_{4+\delta}$, lacking a net defect charge, $\overset{\circ}{Q} = 0$, are *not* spread by Coulomb force but aggregate to $\overset{\circ}{O}\overset{\circ}{O}\overset{\circ}{O}\overset{\circ}{O}$ trains. They give rise to charge-order stripes with with almost constant incommensurability. The doped orbital probabilities $P_{d,p}$ from NQR confirm that the doped holes in $La_{2-x}Sr_xCuO_4$ reside almost entirely at lattice-site oxygen. Likewise, the doped electrons in $Pr_{2-x}Ce_xCuO_4$ are found by NQR to reside almost entirely at lattice-site copper.

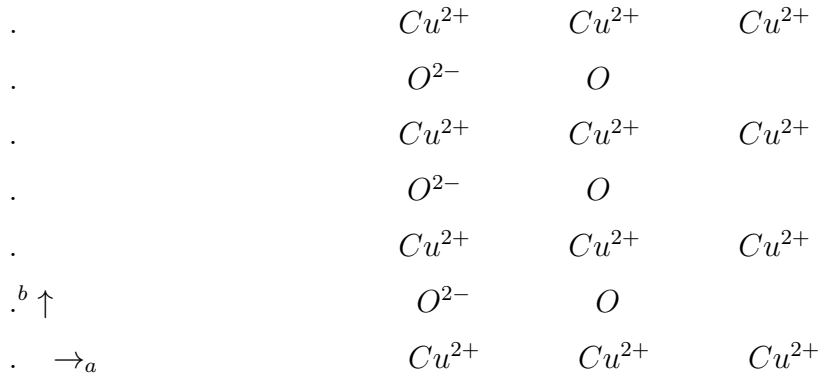
This brings us to the doped-orbital probabilities in $HgBa_2CuO_{4+\delta}$, $P_d \simeq P_p \simeq 0.5$. The NQR formalism by Haase *et al.* assigns doped holes to *lattice-site* ions, Eqs. (1, 2), but makes no allowance for doped O atoms at interstitial sites of the CuO_2 plane. The following diagram shows a doped oxygen atom at the pore position, $\overset{\circ}{O}$, and its planar environment.



The asymmetric positions of its four nearest neighbor O^{2-} ions and four next-nearest neighbor Cu^{2+} ions (all marked bold) give rise to EFG’s at their nuclei and thus to NQR contributions. However, oppositely to hole-doped $La_{2-x}Sr_xCuO_4$, where the changes of NQR are caused by a change of hole density n_p and n_d in O^{2-} and Cu^{2+} orbitals at given EFG’s, Eqs. (6, 5), the changes of NQR in the orbitals of each $\overset{\circ}{O}$ atom’s neighbor ions, O^{2-} and Cu^{2+} , are caused by *changes of the EFG* at essentially constant $n_p \simeq n_{p0}$ and $n_d \simeq n_{d0}$ values. There are four such O^{2-} and Cu^{2+} neighbors to each $\overset{\circ}{O}$ atom with comparable distances and asymmetries. This necessitates a change of interpretation: In $HgBa_2CuO_{4+\delta}$ it is not a “doped-hole” density in the O^{2-} and Cu^{2+} neighbors of $\overset{\circ}{O}$, but the *changed EFG* at their nuclei, that makes the finding $P_p \simeq P_d \simeq 0.5$ plausible. The “doped hole” stays with the

dopant $\overset{\circ}{O}$ atom, representing its open $2p^4$ shell, and contributes to NQR with its self-EFG.

In $YBa_2Cu_3O_{6+y}$, doped oxygen is incorporated (for $y > 0.5$) in both the CuO_2 planes and the CuO chains, Eq. (12). The NQR contributions from $\overset{\circ}{O}$ atoms and their neighbors in the CuO_2 planes are as already illustrated in the above diagram. An example for contributions from the CuO chains, the diagram below gives an ion arrangement in the $Cu(1)$ plane as it may occur for ortho-III oxygen ordered ($y \approx 0.75$), with periodic repetition in the a and b direction. The nearest-neighbor configuration of the O^{2-} ions and O atoms is much more asymmetric than that of the Cu^{2+} ions. Accordingly, much larger EFG's and NQR contributions can be expected from oxygen sites than from copper sites. Added to the essentially equal contributions from oxygen and copper sites in the CuO_2 planes, the finding of $P_p = 0.64$ and $P_d = 0.36$ for $YBa_2Cu_3O_{6+y}$ (Table III) becomes qualitatively plausible.



IX. CONCLUSION

NQR investigations and stripe analysis of high- T_c cuprates complement each other: (i) The small deviation of doped-hole density h from the doping level of $La_{2-x}Sr_xCuO_4$, as observed with NQR, $\Delta h = x - h \approx 0.02$, agrees closely with the density of itinerant holes, \tilde{p} , responsible for suppression of 3D-AFM, as obtained from stripe incommensurability. (ii) The residence of doped holes at oxygen sites in $La_{2-x}Sr_xCuO_4$ and of doped electrons at copper sites in $Ln_{2-x}Ce_xCuO_4$ ($Ln = Pr, Nd$), as assumed in the stripe model, is (to a large degree) confirmed by the NQR studies. (iii) The NQR finding of doped-hole probabilities in oxygen and copper orbitals of oxygen-enriched high- T_c cuprates, $P_p \simeq P_d \simeq \frac{1}{2}$, as well as of oxygen-doped $YBa_2Cu_3O_{6+y}$, $P_p \simeq 2P_d \simeq \frac{2}{3}$, is interpreted with the stripe model in terms

of excess oxygen atoms in the CuO_2 planes and the CuO chains.

- ¹ M. R. Presland, J. L. Tallon, R. G. Buckley, R. S. Liu, and N. E. Flower, *Physica C* **176**, 95 (1991).
- ² J. Haase, O. P. Sushkov, P. Horsch, and G. V. M. Williams, *Phys. Rev. B* **69**, 094504 (2004).
- ³ D. Rybicki, M. Jurkutat, S. Reichardt, J. Haase, “Phase diagram of hole-doped cuprates based on ^{17}O and ^{63}Cu NMR quadrupole splittings,” arXiv:1402.4014
- ⁴ M. Jurkutat, D. Rybicki, O. P. Sushkov, G. V. M. Williams, A. Erb and J. Haase, *Phys. Rev. B* **90**, 140504(R) (2014).
- ⁵ M. Jurkutat, J. Haase, and A. Erb, *J. Supercond. Nov. Magn.* **26**, 2685 (2013).
- ⁶ M. Bucher, “Stripes in heterovalent-metal doped cuprates,” arXiv:2002.12116v7
- ⁷ M. Bucher, “Stripes in oxygen-enriched cuprates,” arXiv:2010.06388v2
- ⁸ N. P. Armitage, P. Fournier, and R. L. Greene, *Rev. Mod. Phys.* **82**, 2421 (2010).
- ⁹ Y. Ohta, W. Koshibae, and S. Maekawa, *Phys. Soc. Japan* **61**, 2198 (1992).
- ¹⁰ E. P. Stoll, P. F. Meier, and T. A. Claxton, *Phys. Rev. B* **65**, 065432 (2002).
- ¹¹ C. Bersier, S. Renold, E. P. Stoll, and P. F. Meier, *J. Phys.: Condens. Matter* **18**, 7481 (2006).